CONULARIID TEST MICROSTRUCTURE AND MINERALOGY

by

ROBERT C. FORD

B.S., Austin Peay State University, 2009

A THESIS

submitted in partial fulfillment of the requirements for the degree

MASTER OF SCIENCE

Department of Geology
College of Arts and Sciences

KANSAS STATE UNIVERSITY
Manhattan, Kansas

2011

Approved by:

Major Professor
Dr. George R. Clark II

Copyright

Abstract

Conulariids are one of the most enigmatic groups of fossil organisms, and have been stimulating debates since the late 19th century. Many major questions remain; for example, three independent researchers (Babcock and Feldman, 1986b; Oliver and Coates, 1987; Van Iten, 1992b) reported three different mineralogies for the conulariid test within a six-year period, and are not known to have reached an agreement. Conulariid morphology is also debated, and many workers seem unable to agree on the basic architecture of the test or how it grows. Conulariid workers have also attempted to determine the taxonomic classification of conulariids, especially whether they have cnidarian affinities or occupy their own phylum.

My work attempts to clarify some of these issues, as well as determine whether any morphological variation exists within single species of conulariids in different paleoenvironments. To this end, I have collected and prepared specimens for examination by scanning electron microscopy, transmitted polarized light microscopy, energy-dispersive spectrophotometery, and x-ray defractometry. Results include evidence for the presence of organic matrix in the conulariid test microstructure, the presence of three types of lamellae in the test, and support for carbonate-rich apatite [$Ca_5(PO_4,CO_3)_3(OH,F)$] mineralogy. Details of the test microstructure add further support for a coronatid scyphozoan affinity. The conulariid species examined here displayed no microstructural or mineralogical variation between different paleoenvironments (unless two of the species are actually environmental varieties, which seem unlikely).

Table of Contents

List of Figures

List of Tables

Acknowledgements

This project would not have been possible if not for the generosity of the Kansas State University Geology Department and alumni. I would like to thank my advisor Dr. George Clark for all of the techniques that I learned, improving my scientific writing skills, and the constructive criticism. My thesis committee deserves a great deal of credit (Dr. Allen Archer, Dr. Saugata Datta, and Dr. Keith Miller) for their input on techniques and ideas to be covered in this project. I need to thank Kent Hampton in the entomology department for his patience and help with the SEM on campus, and Angela Tran in agronomy for my XRD analyses. I want to mention the help and support that I received from my Austin Peay professors, Dr. Daniel Frederick and Dr. Jack Deibert, for allowing me to use their equipment and facilities while I was home during breaks. I really need to thank Dr. Heyo Van Iten at Hanover College for taking time out of his busy schedule to take me to collection sites, for allowing me to use his SEM, and for help with finding hard-to-get literature. Ms. Bushra Hussaini at the American Museum of Natural History in New York City was a big help for allowing me the chance to examine and photograph conulariid specimens housed in their collection. I have to also mention the comic relief supplied to me by my friend Steven Greenwood who traveled with me during my thesis fieldwork, and who took notes and pictures for me as I searched for my fossils. Last, and especially not least, I need to thank Paul and Deanna Strunk for their extremely generous financial support. If not for them the amount of fieldwork, and time that needed to be dedicated may not have been possible.

Dedication

I dedicate this thesis work to my family and friends who have always been supportive of me, and who pushed me to do my very best.

CHAPTER 1 - Introduction

Conulariids are generally accepted as an extinct group of coronate scyphozoans (Phylum Cnidaria) with a geologic range from the Late Proterozoic into the Triassic Period. Conulariids are traditionally thought to be sessile-benthic organisms, but some authors have provided evidence for a possible pelagic lifestyle in mature specimens (Kinderlen, 1937; Moore and Harrington, 1956a). The conulariid test was secreted from the outside inward by ectodermal cells, as evidenced by the inward inflection of the lamellae in the internal carinae (Brood, 1995), and by the presence of epibiotic organisms attached to the test's exterior surfaces during life (Moore and Harrington, 1956a; Van Iten, 1989) (Fig. 1).

The morphological terms used in this paper are consistent with the works of Sinclair (1940, 1942, 1952), Moore and Harrington (1956), Van Iten (1992), and Van Iten et al. (1996). Please refer to Figure 2 in the following discussion.

The conulariid test is generally characterized as having four sides (or faces), a steeply pyramidal form, and a phosphatic composition. The wide end of the test is called the aperture, and the tapering end the apex. The aperture on well-preserved specimens can display lappets that were flexible in life, capable of folding inward to close the aperture. The apical end, if preserved, would either taper into a point or to a schott. A schott is formed when the apex of a conulariid is severed and the animal seals the end with new lamellar shell material (Van Iten, 1991b). A pointed apical end would indicate attachment, and presumably a sessile-benthic, polypoid lifestyle (Moore and Harrington, 1956a; Van Iten, 1991b) (although attachment to a floating substrate cannot be ruled out). The presence of a schott may indicate a mature, pelagic, medusoid lifestyle (Kinderlen, 1937; Moore and Harrington, 1956a), although Brood (1995) argues against this possibility, noting the heavy specific weight of the test and apparent absence

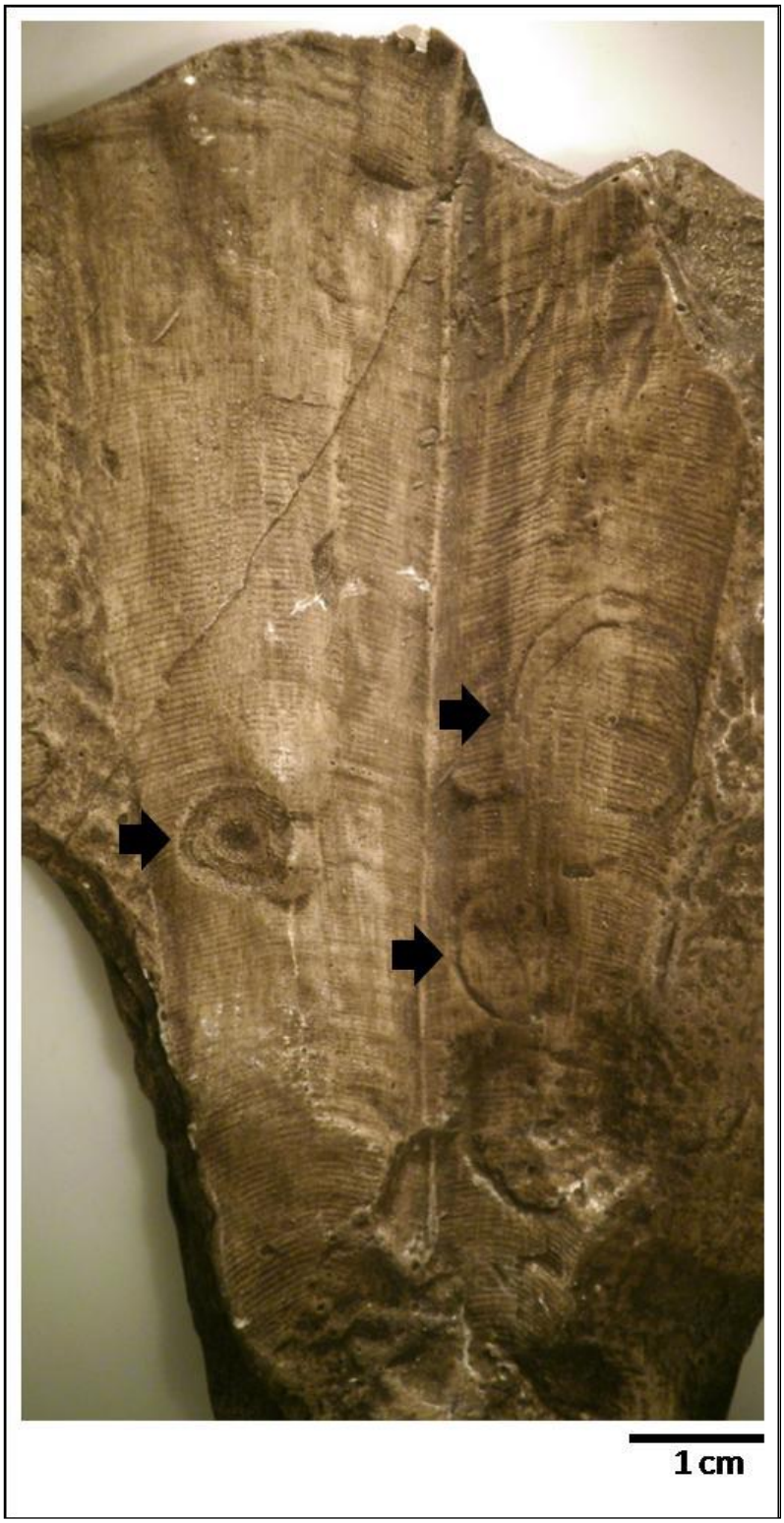

Figure 1- Cast of a conulariid test that displays markings of epibiotic activity (arrows) on the external test surface. Image courtesy of the AMNH FI.

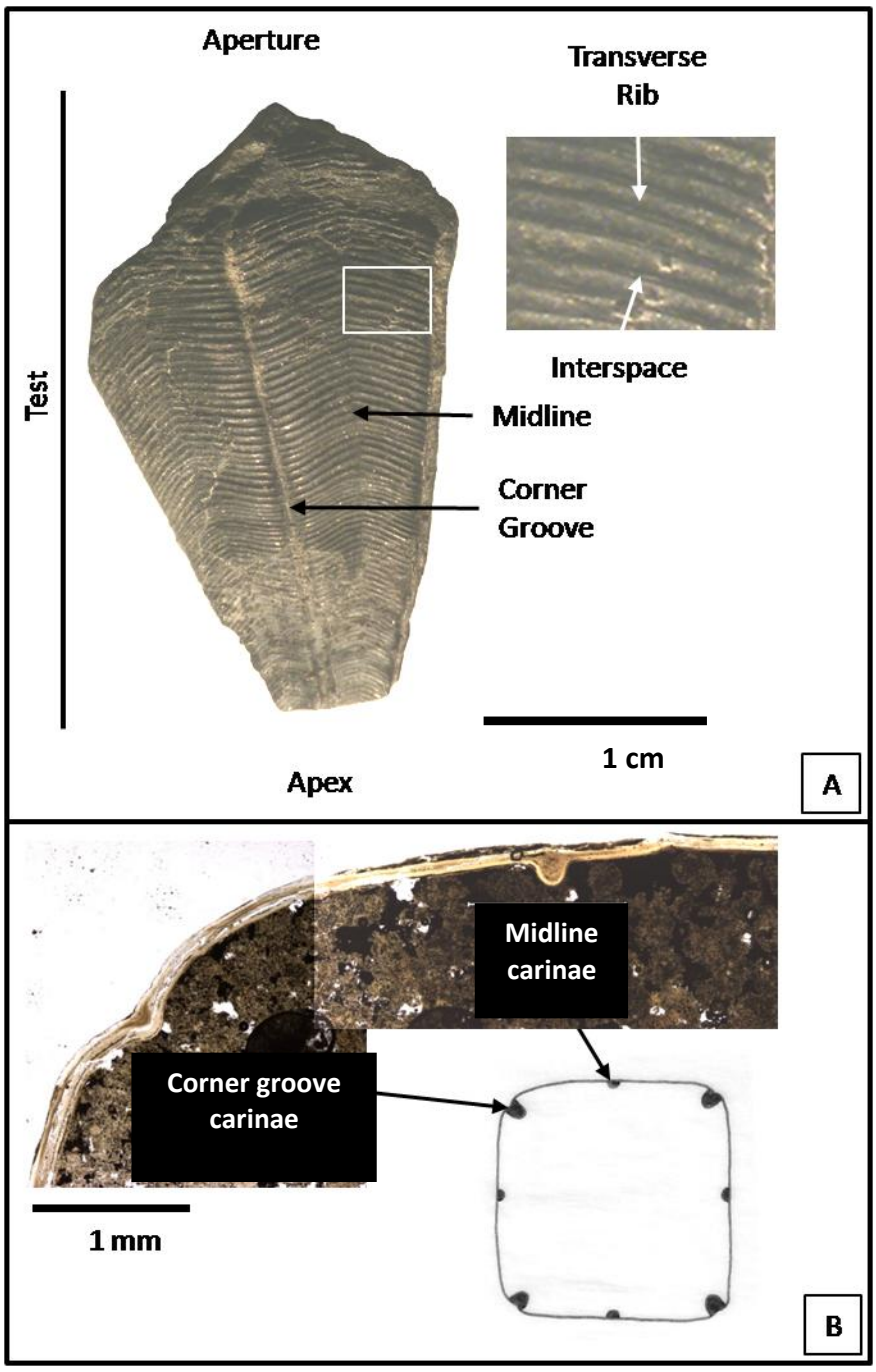

Figure 2- Principal features of conulariid test. A) Surface features. Conulariid test (collapsed) showing external surface of two faces side-by-side, with outlined area enlarged in inset. Visible features include corner groove, midline, transverse rib, and interspace. Image courtesy of the AMNH FI. B) Transverse section through an inflated (not collapsed) conulariid test illustrating laminated microstructure of test and (in section view) two important internal features, a corner groove carina and a midline carina.

of a balancing mechanism. The faces (or sides) of these tests are commonly ornamented with transverse ribs that typically arch toward the aperture at their centers (Moore and Harrington, 1956b; Van Iten, 1992b). The area between two adjacent transverse ribs is called the interspace (Moore and Harrington, 1956b; Van Iten, 1992b). The midline is a longitudinal feature on the conulariid face, sometimes simply the midpoint of the arching ribs, but sometimes more prominent; the midline may be an actual break in the continuity of the ribs, and even mark where the ribs end and become offset, forming more of a chevron pattern than an arch (personal observation). The midlines and corner grooves in some species of conulariids develop carinae (Moore and Harrington, 1956b; Bischoff, 1978; Van Iten, 1991b, 1992a, b, 1996) on the internal test surfaces. The midline carinae follow the same longitudinal path internally as the midline on the exterior test surface. The corner groove is a longitudinal furrow that runs the entire length of the conulariid test. Some species of conulariids also possess internal carinae that develop on the internal surface of the corner groove much the same way as the midline carinae. These corner grooves form where two adjacent faces grew together. The test and all of its features are constructed of phosphatic layers called lamellae that are concordant with the inner test surface (Van Iten, 1992b).

Objectives

The main purpose of this study was to evaluate the hypothesis that conulariid test microstructure and/or mineralogy displays variation within differing paleoenvironments. Subsidiary goals of this study were to make detailed observations of the conulariid test, to (1) determine its mineralogical composition, (2) determine the presence or absence of organic matter, either organic matrix incorporated in mineralized layers, or discrete layers (conchiolin ?)

between mineralized layers, and (3) describe the microstructure of the interspaces, transverse ribs, and internal carinae.

Background

The anatomical features and, to a lesser degree, the mineralogy of the conulariid test have been a consistently debated issue. Many previous authors (Barrande, 1867; Moore and Harrington, 1956a, b; Bischoff, 1978; Steul, 1984; Feldmann and Babcock, 1986; Babcock and Feldmann, 1986a, b; Van Iten, 1991a, b, 1992a, b, 1994; Van Iten and Cox, 1992; Jerre, 1993, 1994; Brood, 1995; Van Iten et al., 1996, 2000, 2005a, b, 2006a, b; Leme et al., 2004) have published on various aspects of conulariid anatomy and morphology. Substantial portions of this anatomical and morphological research have been conducted trying to establish phylogenetic affinities with the morphological features that are associated with the conulariid test. One result of the research is that it has been generally accepted that conulariids constructed their tests by the accretion of fine growth lamellae (Barrande, 1867). More recently Feldmann and Babcock (1986) reinterpreted the construction of the test, suggesting that it is comprised of discreet transverse rods imbedded in a finely lamellar integument. This interpretation was based upon examination of fractured surfaces of specimens with reflected light microscopy and scanning electron microscopy. Van Iten (1991b, 1992a, b), Jerre (1994), and Brood (1995) rejected that interpretation, and presented more evidence for the construction of conulariid tests from continually grown lamellae, by examining polished sections through transverse ribs in the test, equivalent to Feldmann and Babcock's (1986) transverse rods. The internal carinae of the conulariid test have also received mixed interpretations of formation and function. The internal carinae were formed from local inflections of the tests' inner lamellae (Reed, 1933; Bouček,

1939; Van Iten, 1991a, 1992a). The internal carinae present at the corner grooves and midlines have been interpreted as former sites of gastric septum or musculature attachments (Kinderlen, 1937; Moore and Harrington, 1956a, b; Werner, 1966a, b, 1967; 1937; Moore and Harrington, 1956a, b; Werner, 1966a, b, 1967; Bischoff, 1978; Van Iten, 1991a, 1992a). Challenges to this interpretation have been various and flawed. For example, Stuel (1984) misidentified conulariids as orthocone cephalopods, and others (Feldmann and Babcock, 1986; Babcock and Feldmann, 1986a) misinterpreted the internal carinae as taphonomic artifacts.

Conulariid test mineralogical composition has met with little agreement among authors (Moore and Harrington, 1956a; Babcock and Feldmann, 1986b; Oliver and Coates, 1987; Van Iten, 1992b). Their only consistent observation is that the test is comprised of some sort of phosphatic material. Moore and Harrington (1956a) and Oliver and Coates (1987) reported a chitinophosphatic composition of the conulariid test. Chitinophosphate is an organic material formed from chitin, which is either impregnated by or layered with phosphatic mineralization. Babcock and Feldmann (1986b) reported apatite [$Ca_5(PO_4)_3(OH,F)$] as the primary component of the conulariid test, while Van Iten (1992b) reported that it was carbonate-rich apatite [$Ca_5(PO_4,CO_3)_3(OH,F)$]. Carbonate-rich apatite (formerly called carbonate-apatite) is formed when carbonate ions are incorporated into an apatitic crystalline structure, usually substituting for a phosphate ion or but sometimes located in the C-axis anion channel (Dosen, 2009).

Stratigraphy and Depositional Environments

Specimens of two genera of conulariids have been collected in equivalent environments of different ages (Appendix A). *Conularia trentonensis* and *C. splendida* specimens (Fig. 3, A & B) were collected from the Elgin Member of the Maquoketa Formation (Richmondian,

Ordovician) in northeastern Iowa and southeastern Minnesota. *Paraconularia sp.* and *P. missouriensis* specimens (Fig. 3, C & D) were collected from the Fort Payne Formation (Osagean, Mississippian) in central Tennessee. The conulariid distributions in both the Elgin Member and Fort Payne Formation are facies dependent: *Conularia trentonensis* (Van Iten et al., 1996) and *Paraconularia sp.* are found in basinal sediments of their respective geological units, and *C. splendida* (Van Iten et al., 1996) and *P. missouriensis* are both associated with shelf-slope deposits (Fig. 4). These geological units were selected for their analogous depositional environments and conulariid distributions for a comparative study.

Elgin Member, Maquoketa Formation

The Elgin Member represents a shallowing-upward sequence in Iowa and Minnesota (Witzke, 1980, 1987) (Fig. 5, A). The portions of the formation that represent the shallowest depositional setting are located in southeastern Minnesota, and are characterized by an abundance of carbonate deposition. The portions of the formation that represents the deepest depositional settings are located in east-central Iowa and are notably more siliciclastic (Witzke, 1980, 1987). The lithologic and depositional descriptions are consistent with the works of Witzke (1987), Witzke and Glenister (1987), and Raatz and Ludvigson (1996).

Conularia splendida specimens were collected from the outer shelf-slope deposits of northeastern Iowa around Clermont and Elgin. These sediments alternate between thin-bedded carbonates and shales (Raatz and Ludvigson, 1996). *Conularia trentonensis* specimens were collected from basinal deposits in east-central Iowa in Graf. The lithology present at this location is predominately black to brown phosphatic shales, which produced the conulariids, and are overlaid by thick carbonates interbedded with thin shales (Witzke and Glenister, 1987; Raatz and Ludvigson, 1996).

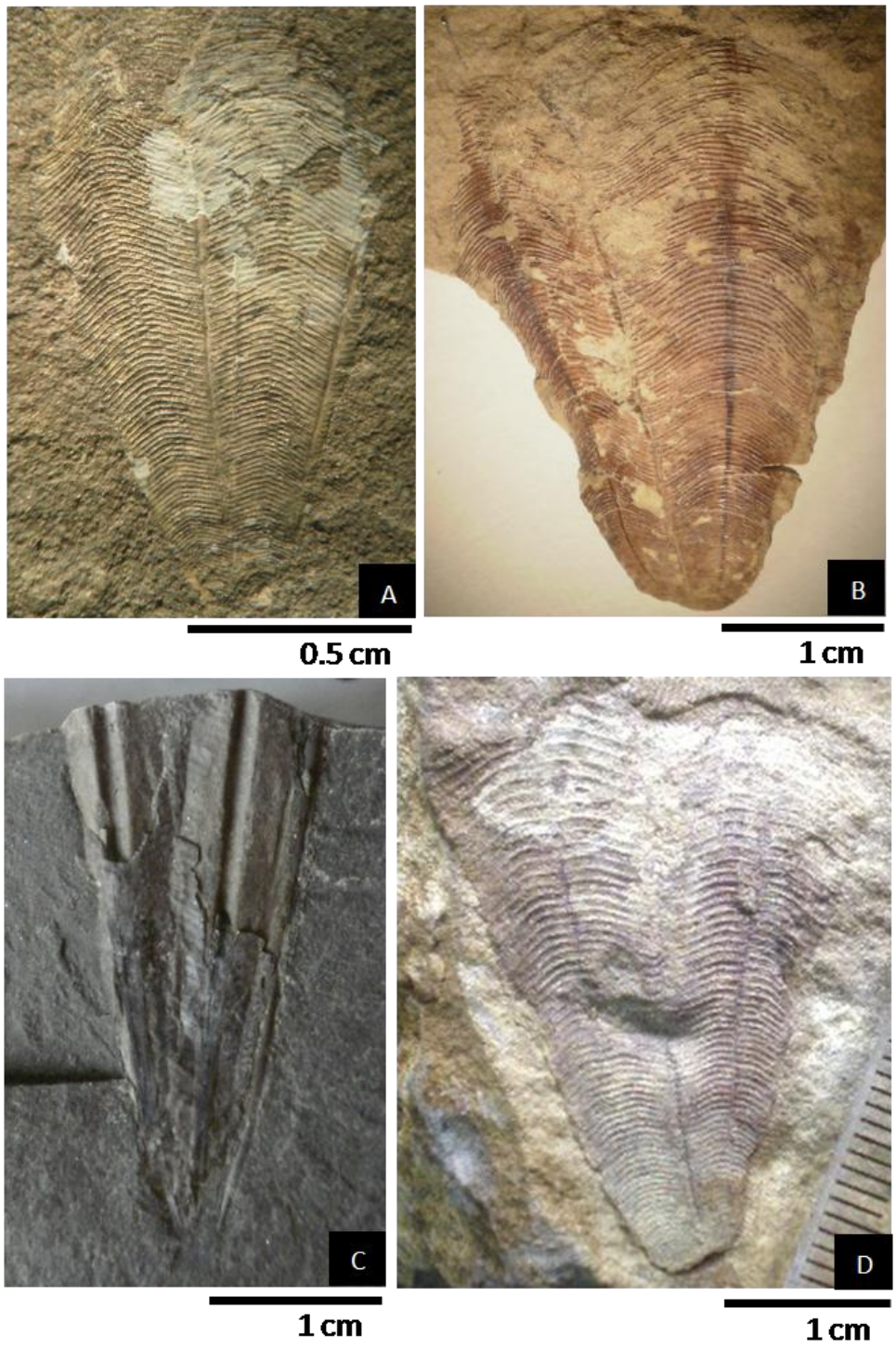

Figure 3- Images of the four conulariid species in this study. A) *Conularia trentonensis* (external surface of two faces of collapsed specimen); B) *Conularia splendida* (external surface of two faces of partially collapsed specimen); C) *Paraconularia* sp. (external surface [bottom half] and internal mold [top half] of two faces of collapsed specimen); D) *Paraconularia missouriensis* (external surface of two faces of collapsed specimen). Note differences in scale.

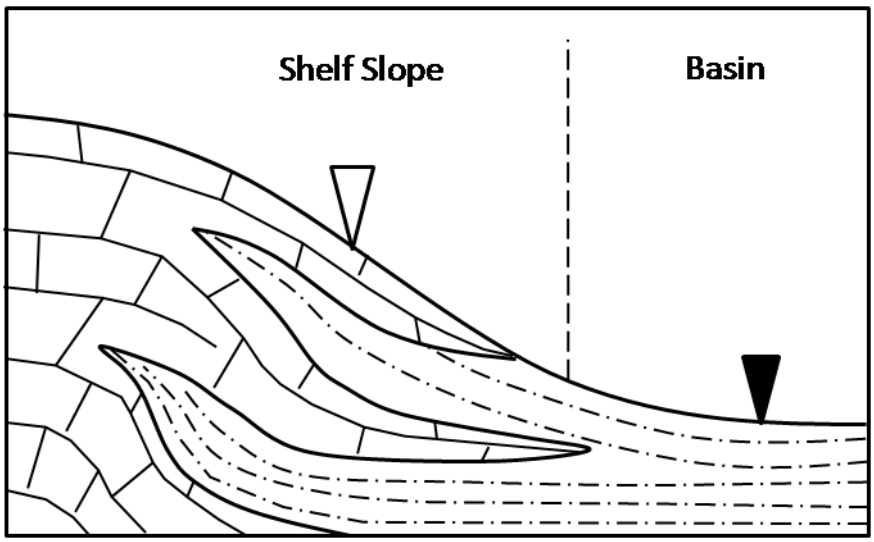

Figure 4- Diagram showing depositional environments from which conulariid specimens were collected for this study. The black triangle represents the position of *Conularia trentonenesis* and *Paraconularia splendida*. The white triangle represents the position of *Conularia splendida* and *Paraconularia missouriensis*.

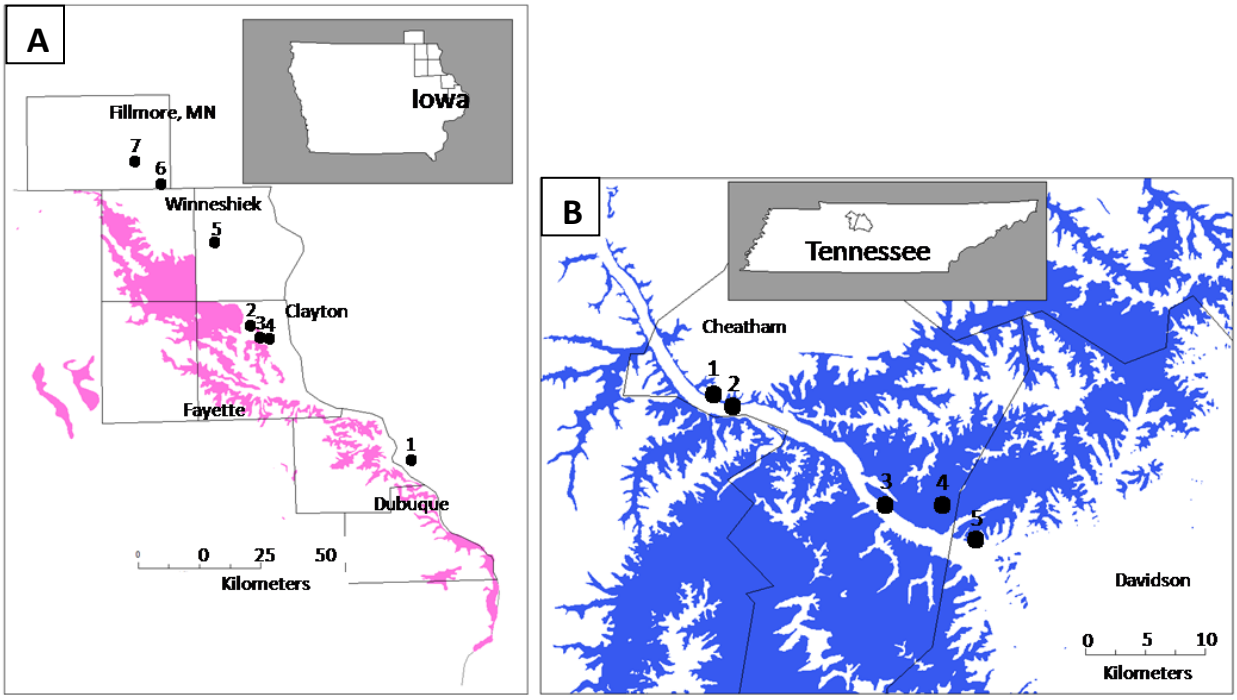

Figure 5- Outcrop areas and collecting sites for this study. For details, see appendix A. A) Elgin Member of Maquoketa Formation (Richmondian, Ordovician) in Iowa and Minnesota. B. Fort Payne Formation (Osagean, Mississippian) in a part of Tennessee.

Fort Payne Formation

The Fort Payne Formation represents a progradational, shallowing-upward, basin-filling sequence (Pryor et al., 1974; Lewis and Potter, 1978; Meyer et al., 1989; and Ausich and Meyer, 1990) deposited from northwestern Georgia to southern Illinois (Ausich and Meyer, 1990) during the Early Mississippian. The Fort Payne Formation outcrops observed in Tennessee (Fig. 5, B) are consistent with the lithological descriptions of Meyer et al. (1989) and Ausich and Meyer (1990) of south-central Kentucky and north-central Tennessee. It is dominated by siliclastic deposition from reworked sediments of the Borden Delta (to the north in Kentucky) (Krause and Meyer, 2004), with carbonate deposition becoming locally common in the upper part of the formation.

Paraconularia missouriensis specimens were collected from shelf-slope deposits of the upper Fort Payne Formation near Cheatham Dam in central Tennessee. The outcrop lithology is predominately siltstone, commonly interbedded with crinoidal sheet-like packstones (Meyer et al., 1989; Ausich and Meyer, 1990). *Paraconularia sp.* specimens were collected in basinal deposits in the lower Fort Payne Formation around Ashland City and Scottsboro Tennessee. The outcrop lithology is primarily dark gray shales.

CHAPTER 2 - Methods and Materials

Sample Selection

Representative specimens were selected from each of the studied species (*Conularia trentonensis*, G08, G11; *C. splendida*, CC01, MH02; *Paraconularia sp.*, RB01, RB05; *P. missouriensis,* RB06, RB07, RB08) for their quality of preservation. These displayed no

apparent structural and chemical alteration within their tests, and are interpreted as having original shell material.

Sample Preparation

Specimens selected for study were embedded in epoxy to prevent loss of surface material and to stabilize the matrix. A number of transverse and longitudinal sections were cut from each specimen. These were further prepared as thin sections for transmitted light microscopy, and as polished and etched sections for scanning electron microscopy (SEM). See Appendix B for a list of prepared material.

The thin section material was ground flat, cemented to glass slides, cut into thin wafers on the slides, and then ground until transparent; no effort was made to achieve standard thickness. Cover slips were applied using immersion oil to permit removal for further analysis if desired.

Specimens for scanning electron microscopy were prepared by cementing transverse and longitudinal sections to aluminum mounts. They were then ground, polished, and cleaned ultrasonically. Because there were many uncertainties regarding the presence and distribution of organic matter, the mounts were next etched and subjected to critical point drying procedures to preserve acid-resistant organic matter in its normal relationship to the mineralized portions of the test.

Following the procedures outlined by Clark (1980), the stubs were soaked in distilled water for sixty seconds and etched in dilute (0.1 N HCl) for 15 to 60 seconds. From this point on, all transfers from one solution to another were done holding the etched surface horizontal; this maintained a meniscus on the surface of the stubs and prevented soft structures from

collapsing under surface tension. The stubs were removed from the acid, sequentially immersed in two purified water baths for a minimum of sixty seconds each, and then sequentially immersed in a series of ethanol solutions of 50%, 75%, 95%, and 100% for sixty seconds each. The critical point dryer's chamber was filled with a 100% ethanol and the stubs placed and sealed inside.

The chamber was purged with liquid CO_2 for four minutes, and then soaked with CO_2 for four minutes. That cycle was repeated four times. On the final cycle a container of water was heated to 45°C. The chambers' source of CO_2 was shut off; then the chamber was immersed in the warm water to reach critical point at around 1400 psi. The critical point was maintained for at least ten minutes to equilibrate. After this, the CO_2 was slowly bled off, allowing at least one minute for each 300 PSI pressure drop, both to prevent uneven pressure changes in fractures and to reduce any turbulence along the surfaces.

To verify whether some surface features exposed by this method would be organic, and presumably weak and flexible, some mounts were air dried after being etched and rinsed by distilled water instead of being critically point dried. If a soft organic matrix is present, then it should collapse and form a gelatinous mat from the pressure of the surface tension of the water as it dried. If organic matter is not present then the air dried mounts would appear the same as the mounts that underwent critical point drying.

Following drying, the specimen mounts were stored in a low-humidity environment to prevent deterioration of the organic matrix. Before being put into the SEM the mounts were coated with gold-palladium to further protect the organic matrix and prevent electron buildup on the stub surface.

Samples for x-ray diffraction were prepared by grinding and sieving to achieve a powder with a particle size less than 53 μm.

CHAPTER 3 - Results

Microstructure

Organic Matrix

Scanning electron microscopy of the critical-point dried specimens revealed an abundance of organized structures, apparently organic matrix, within the microstructure of conulariid tests (Fig. 6). Examination of air-dried comparison material (see Sample Preparation, above) revealed collapsed, apparently gelatinous mats (Fig. 7), demonstrating the organic nature of this matrix material. Specimens of each species (G08, MH02, RB05, and RB08) were tested in this way, and each indicated preservation of the organic matrix.

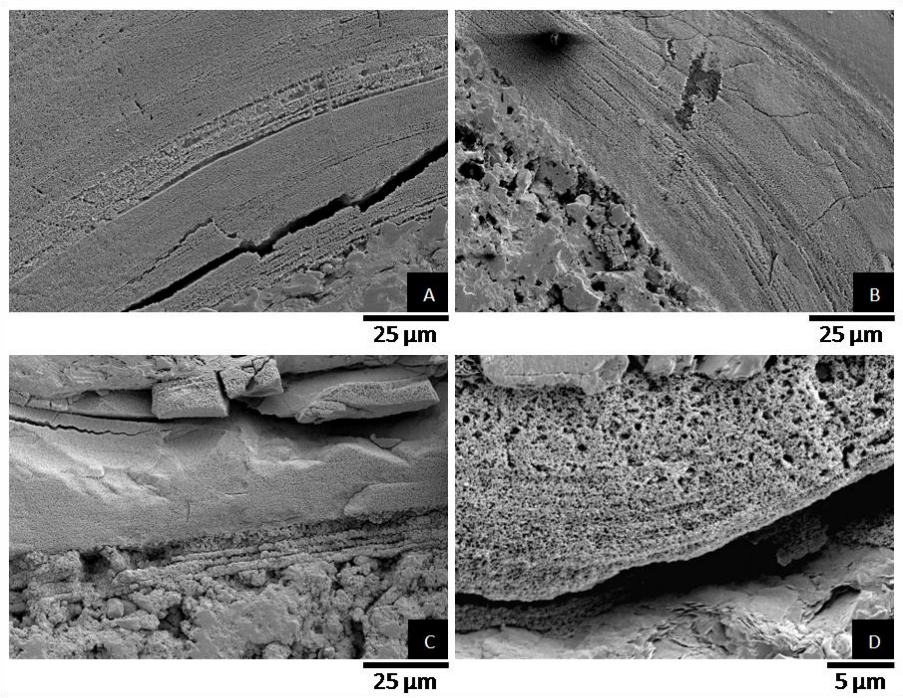

Figure 4- Sections through conulariid tests, showing distribution of organic matrix at surface revealed by etching and critical point drying. Note that nearly the entire surface of the sections have abundant matrix, with variations in abundance corresponding to positions of the microlamellae. A) Specimen RB05, *Paraconularia* sp.; B) Specimen RB08, *Paraconularia missouriensis*; C) Specimen MH02, *Conularia splendida*; D) Specimen G08, *Conularia trentonensis*. Scanning electron micrographs.

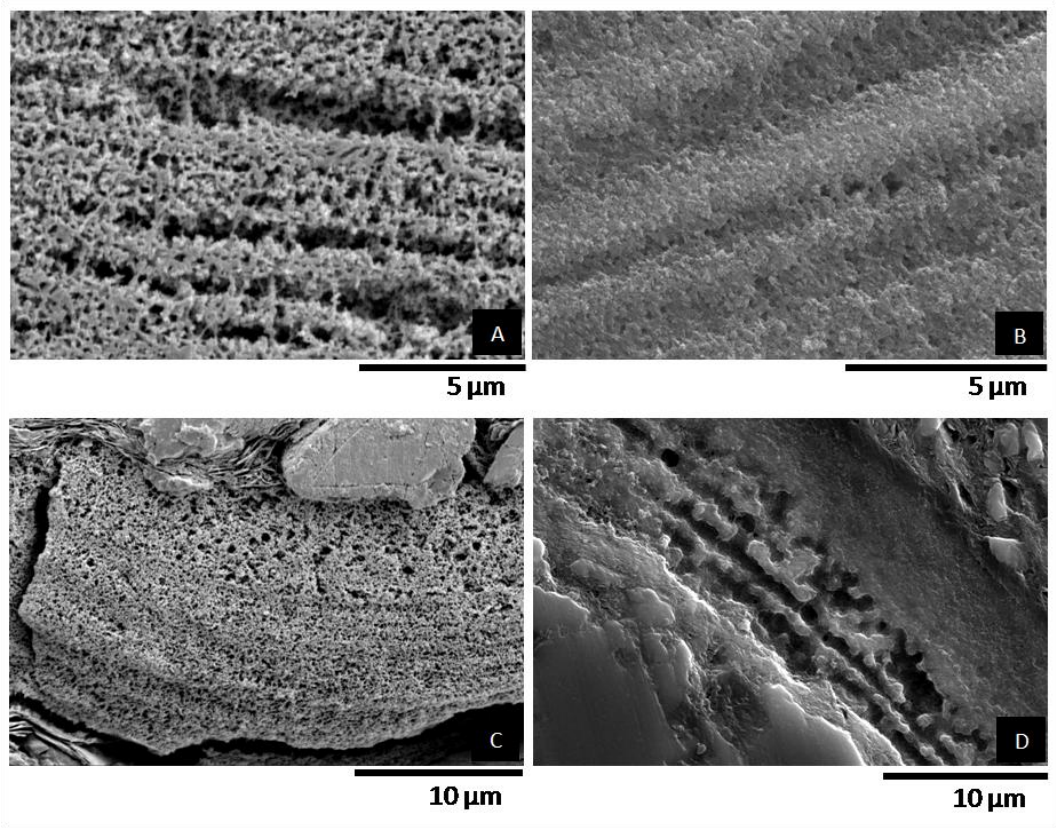

Figure 5- Sections through conulariid tests, showing the organic matrix exposed by etching. Images (A) and (B) are of specimen RB08 (*Paraconularia missouriensis*), while (C) and (D) are of specimen G08 (*Conularia trentonensis*). Images (A) and (C) have been prepared by critical-point drying, while (B) and (D) are air dried. These comparisons show that the organic matrix exposed in each species is soft enough to collapse under the pressure of surface tension, and is presumably the original organic material. Scanning electron micrographs.

Microlamellae

Knowing that an organic matrix is preserved in these conulariid tests permits further observations and interpretations of the microstructures. In all four etched tests (specimens RB05, RB08, G08, and MH02), the organic matrix is largely confined to very thin (0.30 µm to 1.25 µm) lamellae, with etching patterns suggesting low proportions of mineralized material. These organic-rich lamellae are separated by gaps of very similar thickness with occasional thin strands of organic matrix running across them (Fig. 8). These gaps presumably represent organic-poor, heavily mineralized lamellae, although the proportion of organic matrix once within them cannot be determined, as it probably included some material lost during etching. I

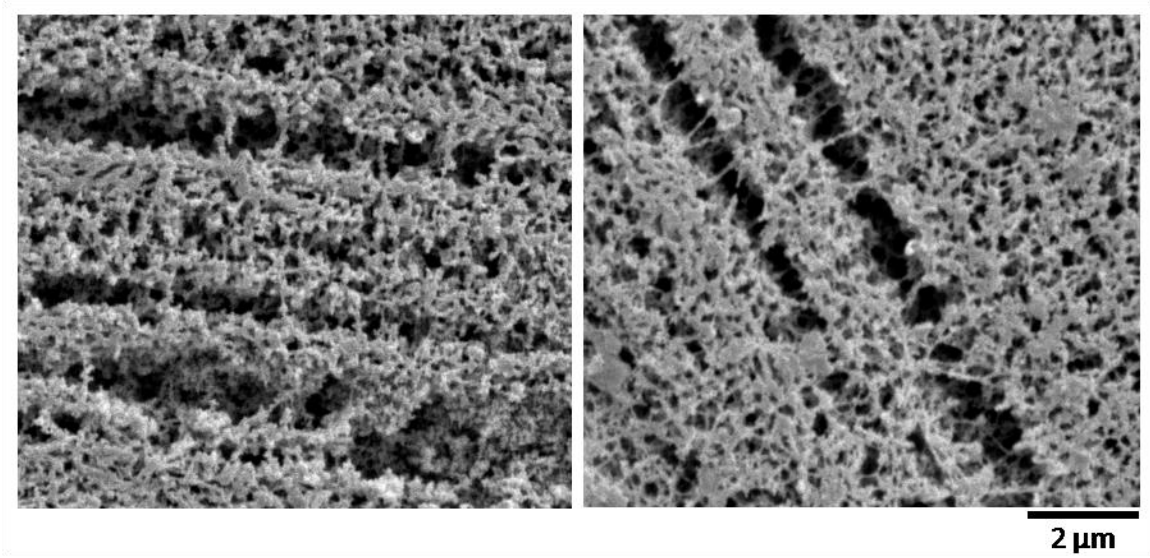

Figure 6- Sections through conulariid tests, showing details of the microlamellae exposed by etching and critical-point drying. Variations in organic content of individual microlamellae are frequent and sometimes very obvious; some microlamellae seem to have been almost completely mineralized, with the only evidence that they were not fractures being the occasional strands of matrix that cross the gaps left by the etching. A) Specimen RB05, *Paraconularia* sp.; B) Specimen RB08, *Paraconularia missouriensis*. Scanning electron micrographs.

will refer to these types of thin lamellae as *microlamellae*, organic-rich and organic-poor. Such patterns of calcification have been noted in numerous studies on periodic growth and growth lines (see, for example, Clark, 1974, 1999).

The microlamellae remain parallel or sub-parallel in both transverse and longitudinal sections, as can be seen in Figure 9. The organic-rich microlamellae do not commonly display much variation in thickness along longitudinal and transverse sections. However, the organic-poor microlamellae sometimes display significant variations, sometimes doubling in thickness, in both directions. It appears as if the conulariid thickened its test by increased mineralization and organics in the transverse ribs and internal carinae. One type would thicken and the other type would not and this alternated between both organic-rich and organic-poor microlamellae.

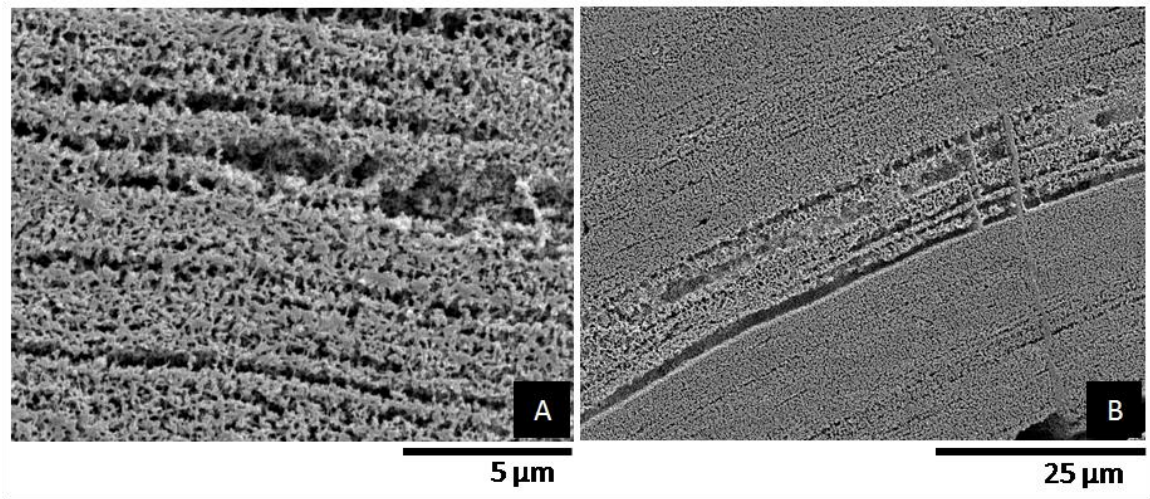

Figure 7- Etched and critical-point dried sections through the test of specimen RB05, *Paraconularia* sp. A) Transverse section; B) longitudinal section. Note how the microlamellae remain parallel and nearly constant distances apart across the sections. Scanning electron micrographs.

Mesolamellae

I apply the term *mesolamellae* to a type of lamellar structure observable only in crossed polarized, transmitted light microscopy. When the thin sections were examined under crossed polarized light the mesolamellae became visible, and appear to be distributed throughout the conulariid test (Fig. 10). These lamellar structures are present in all the examined specimens, and generally range from 5 µm to 15 µm in thickness. They can vary in thickness along both transverse and longitudinal sections. Two types of mesolamellae can be distinguished, transparent and dark; these alternate with each other throughout the entire thickness of the conulariid test (Fig. 11). The mesolamellae are presumed to be groupings of microlamellae of similar characteristics. Both light and dark types display extinction at 90°, although this is more obvious in the light layers. The lighter layers probably have less concentrated organic matter (presumed groupings of organic-poor microlamellae), and thus more, and perhaps more organized crystal structure. The darker mesolamellae seem to have a higher concentration of organics (presumed groupings of organic-rich microlamellae), which are partially blocking the

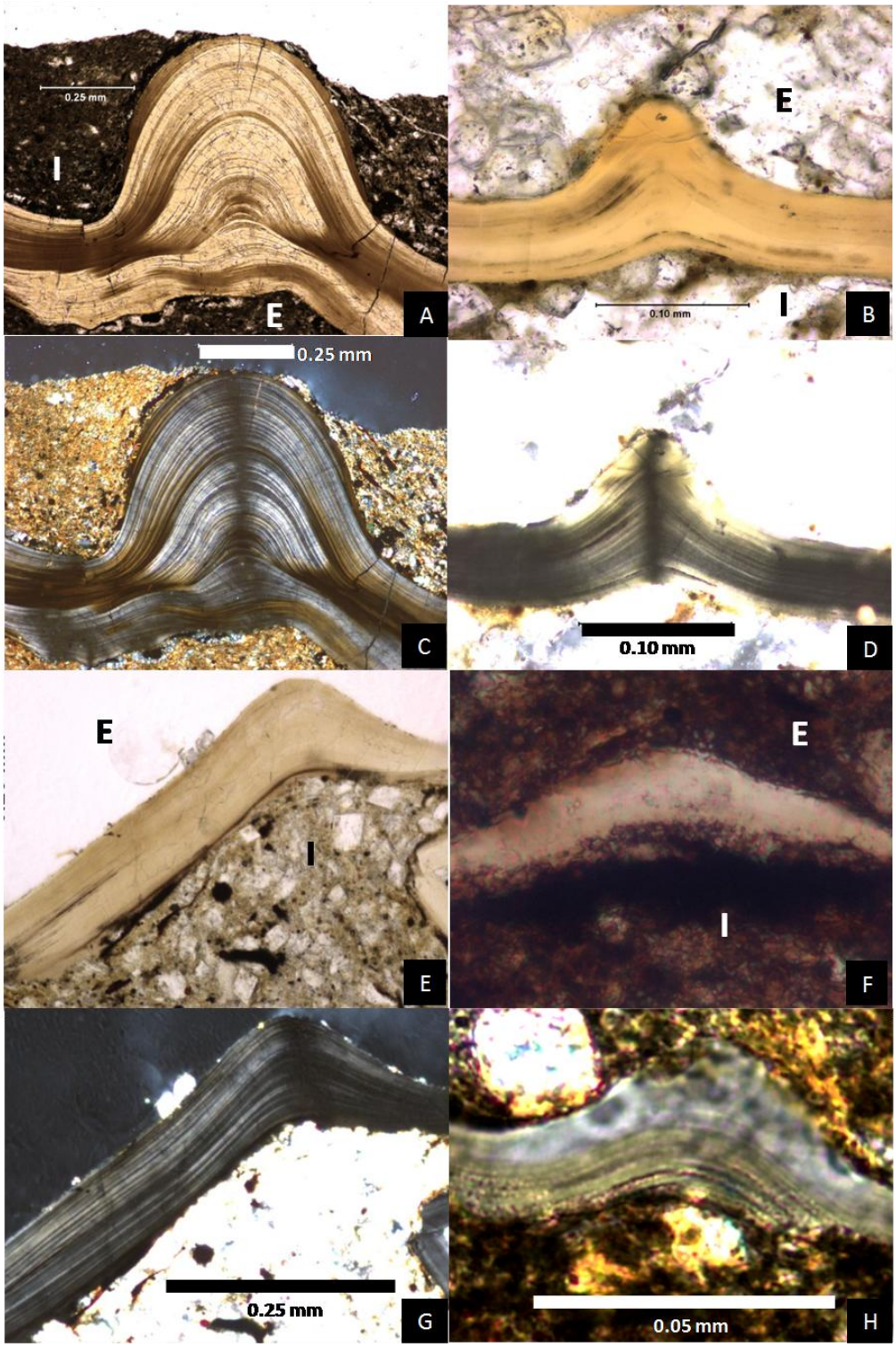

Figure 8- Thin section preparations of sections through conulariid tests viewed with light microscopy; images (A), (B), (E) & (F): plane polarized; images (C), (D), (G) & (H): crossed polarized. The mesolamellae are readily seen in the crossed polarized images. A&C) transverse sections through the corner groove carina of specimen RB05 (*Paraconularia* sp.). B&D) longitudinal section through a transverse rib of specimen CC01 (*Conularia splendida*). E&G) longitudinal section through a transverse rib of specimen RB08 (*Paraconularia missouriensis*). F&H) longitudinal sections through different transverse ribs of specimen G08 (*Conularia trentonensis*). **(**E = external; I = internal)

transmitted light and therefore contain a lesser amount of biomineralization. Specimens RB01 and RB05 displayed one further difference in their mesolamellae. In these, although both light and dark layers show extinction at 90°, the extinction points are offset from each other by 45°. Except for RB08, where a lack of material precluded a transverse section, the extinction patterns for each species were the same in longitudinal and transverse sections.

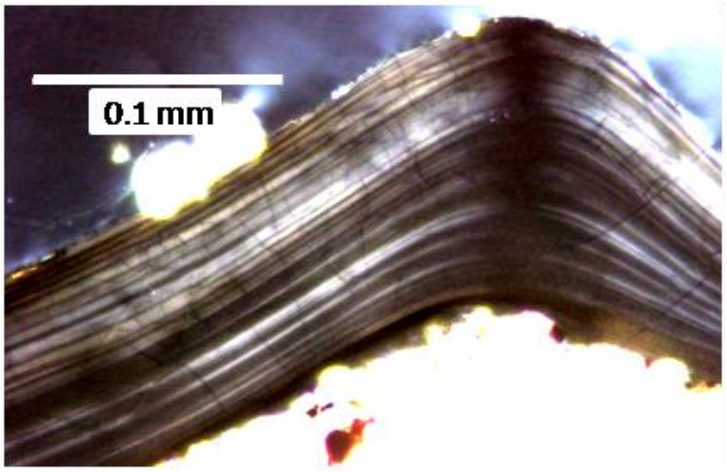

Figure 9- Longitudinal section through a transverse rib of specimen RB08 (*Paraconularia missouriensis*), displaying an alternating pattern of light and dark colored mesolamellae. Crossed polarized light.

Macrolamellae

Macrolamellae are relatively large lamellar structures that are visible at several different magnifications, and, probably represent all lamellae described in older, pre-SEM investigations. These lamellar structures are not readily observed in conulariids with thin tests (G08, G11, CC01, MH02, RB06, RB07, and RB08), and not every study has reported them. However, Paraconularia sp. (RB01 and RB05), which possesses the thickest test examined in this study, displays obvious alternating dark (brown) and light colored lamellar structures ranging from 5 µm to 75 µm in thickness. Single macrolamellae can vary in thickness in both transverse and longitudinal sections. The thicknesses and patterns examined in the macrolamellae of the thick-test specimens (RB01 and RB05) also differ greatly among individual specimens of the same species (see Figure 12). In specimen RB01 the macrolamellae are roughly equal in thickness and are continuous in transverse and longitudinal sections. In specimen RB05 they vary in thickness

and have less continuity, especially the dark brown macrolamellae seen in test thickenings. Interestingly, these macrolamellae appear to have a relationship with the mesolamellae. In specimen RB01 they overlay almost exactly with a very tight correlation. Specimen RB05 also shows this, but the correlation is not as exact (Fig. 13).

Test Features and Growth

It seems clear that the conulariid test is secreted by the ectodermal cells of the animal (see Moore and Harrington, 1956a; Van Iten, 1989), and that the secretion is more or less continuous along the entire interior surface of the test. From this observation we can conclude that any ornamentation on the exterior of the test is related to folds in the ectoderm as the initial lamella is produced (and as new lamellae form extensions to the test during growth). In contrast, any features on the interior of the test that are not parallel to the exterior surface must be formed by variations in the thickness of new lamellae at those points.

Here I will discuss interior features for which new lamellae are not parallel to the exterior lamellae. Three such features (interspace, transverse ribs, and internal carinae) were selected for study, because of their commonality and the ease of their identification. The specimens examined did not have any healed injuries, nor did they have a schott preserved, thus implying that the studied features were produced during normal growth.

Interspace

The interspaces are externally expressed on the test as the lowered features that are, more or less, horizontally oriented regions between the raised transverse ribs. In this region the lamellar structures are the most parallel and most concentrated. This area is also more organic-rich than other parts of the test. The organic-poor microlamellae are thinnest in the interspaces;

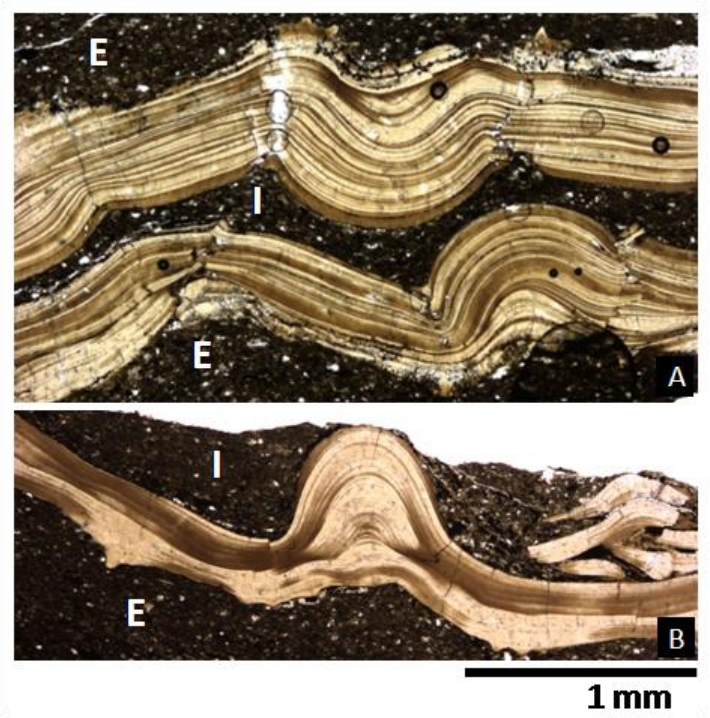

Figure 11- Thin section preparations of transverse sections of conulariid tests viewed with light microscopy; both images are viewed in plane polarized light. A) specimen RB01 (*Paraconularia* sp.) (collapsed, showing two corner groove carinae nearly touching each other). B) different specimen (RB05) of the same species, with one corner groove carina visible. Note that RB01 has a much more uniform distribution of the macrolamellae. (I = interior, E = Exterior)

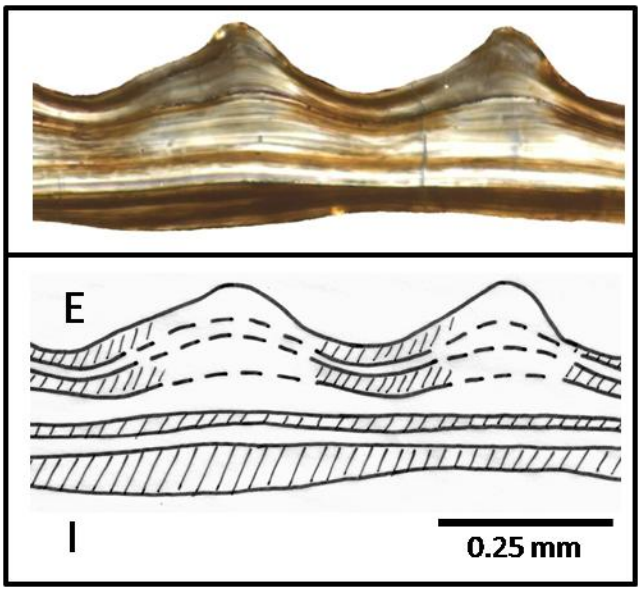

Figure 10- Thin section preparation of longitudinal section through two transverse ribs of specimen RB05 (*Paraconularia* sp.), viewed with light microscopy (plane polarized light). Lamellar boundaries demonstrate that new lamellae deposited on the inner surface (I = internal; E = external) are thicker at the ribs and fill them in over time, evening out the inner surface. (hachures on lower diagram indicate organic-rich lamellae; clear areas between them indicate organic-poor lamellae.)

the organic-rich microlamellae are much the same in thickness here as elsewhere, so they make up more of the whole. The mesolamellae and macrolamellae both typically do not show much variation in thickness along the individual lamellae in the interspaces.

Transverse Rib

The transverse ribs are externally expressed test thickenings. These features are the raised ridges on the faces of the conulariid test. Throughout the growth history of a conulariid it appears that subsequent lamellar structures are individually thicker at the ridges than at the interspaces, so that the internal test surface becomes less 'wrinkled' than the external test surface (Fig. 13). The thickening reached down to the microlamellar scale; no new microlamellae were added specifically to this region. However, the thickening of microlamellae was sometimes more obvious within the organic-poor varieties, and sometimes more obvious within the organic-rich varieties (Fig. 14). This can give the structures the appearance of 'feathering' as the microlamellae approach the rib.

The mesolamellae are typically more continuous through the ribs. The light and dark colored mesolamellae both expand in the transverse ribs. Thickening of these lamellae appears to be the primary mode of forming the ribs although some 'feathering' is observed (Fig. 15). This may be an expression of thickening in organic-poor microlamellae, or the organic-rich variety may be condensing to give a 'feathering' effect in the mesolamellae. Mesolamellae that fan out as they approach the rib typically converge again on the opposite side (Fig. 15).

The macrolamellae displayed a variety of behaviors. In specimen RB01 the macrolamellae, both light and dark, are difficult to identify in the transverse rib due to some dissolution between the ribs. But in specimen RB05 the dark macrolamellae fan out and seem to

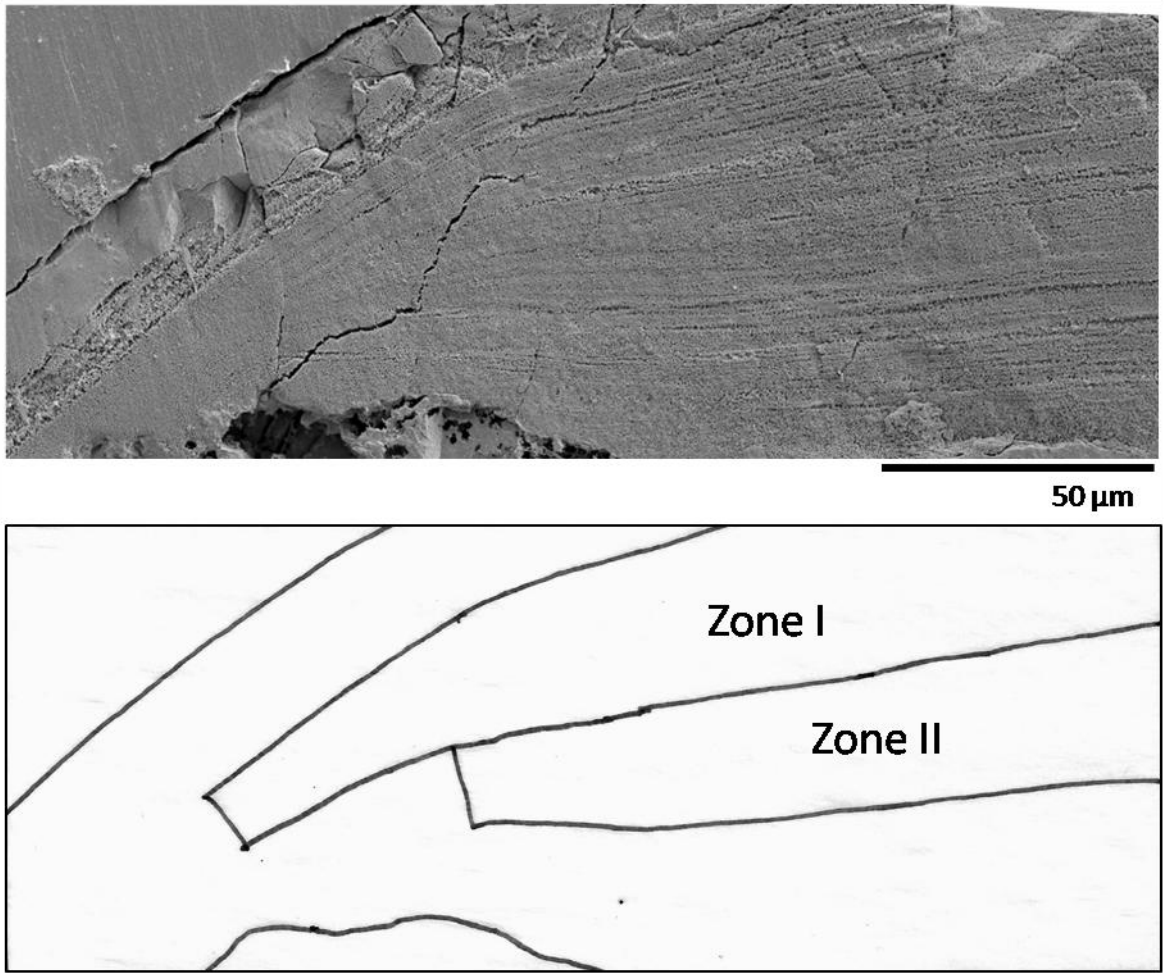

Figure 12- Longitudinal section through a transverse rib of the test of specimen RB08 (*Paraconularia missouriensis*), showing patterns of microlamellae as seen in organic matrix revealed by etching and critical-point drying. In the interspace at the left the microlamellae are thin and tightly packed, while in the rib they show thickening and greater diversity with respect to organic content. In the area marked 'Zone I' on the lower diagram there are more prominent 'gaps' (interpreted as organic-poor microlamellae that are etched out of sight), while in 'Zone II' the lesser number of 'gaps' suggests that more of the microlamellae are organic-rich, suggesting a slower rate of mineralization. Scanning electron micrograph.

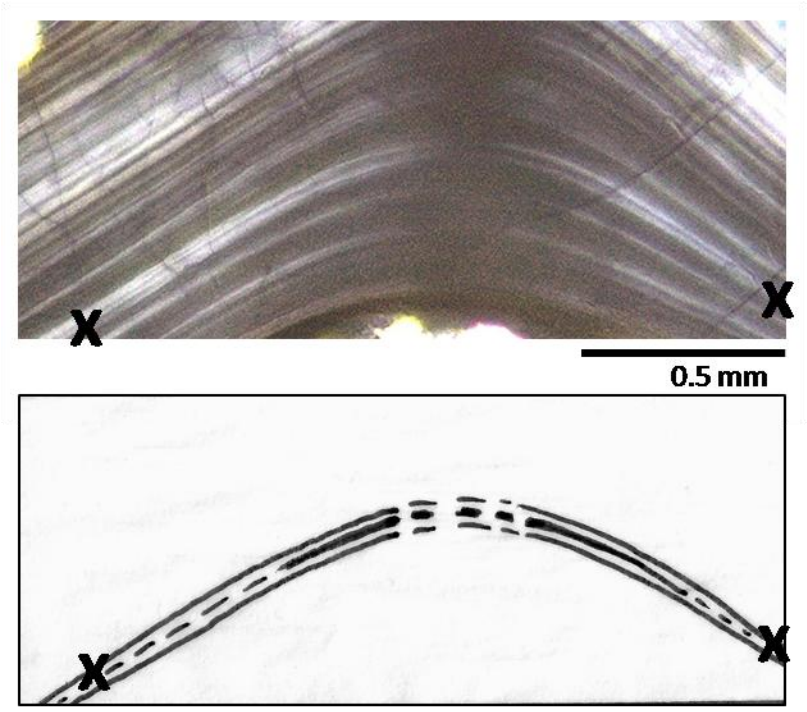

Figure 13- Thin section preparation of a longitudinal section through another transverse rib in the test of specimen RB08 (*Paraconularia missouriensis*), showing how some mesolamellae can appear to 'split' due to the increased thickness of an organic-rich layer in the center of the rib. 'X' marks either end of an organic-poor mesolamella that shows this effect. Transmitted light microscopy, crossed polarized light.

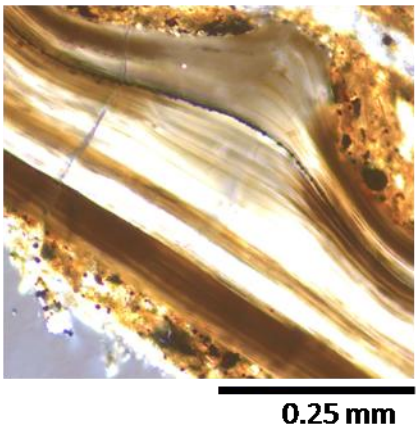

Figure 14- Thin section preparation of a longitudinal section through a transverse rib in the test of specimen RB05 (*Paraconularia* sp.), showing that the upper two macrolamellae appear dark in the interspaces (on both sides) and appear almost transparent where they are adding to the thickness of the rib (center). This is interpreted as showing that the rib thickening involves an increase in mineralization, while organic matrix growth remains constant, so the darkness of the matrix is 'diluted' at the center. Note that the last macrolamella to form (at bottom) remains a constant dark shade, presumably because there is no thickening of the rib by that lamella. Transmitted light microscopy, plane polarized light.

disappear in the transverse ribs just to taper back together and reappear on the opposite side. On the other hand the light macrolamellae appear to thicken (Fig. 16). This is presumably because of the diffusion of the organics and a higher concentration of mineralization within the rib, reducing the proportion of organic content in the center.

Internal Carina

Internal carinae are internally expressed test thickenings. As previously mentioned they are associated with the corner grooves and/or midlines, which externally are sunken or flat. Unlike the transverse ribs that were filled internally by the growth of new lamellae, internal carinae are formed by the thickening and subsequent inflection of lamellae on the smoother internal test surfaces (Fig. 17). Otherwise the behaviors of the lamellar structures (microlamellae, mesolamellae, and macrolamellae) in the construction of the internal carinae are much the same as what was described for the transverse ribs

Mineralogy

X-ray diffractometry (XRD) analysis on specimen RB09 (*Paraconularia sp.*) was accomplished on two samples: fragments of the matrix around the conulariid, and fragments of the conulariid test with some attached matrix material. When the two analyses are compared, the fossil + matrix sample appeared to have one set of peaks different from the matrix sample. These fossil + matrix peaks suggest the presence of carbonate-rich apatite (Fig. 18). The other, thin-test conulariid species could not provide an adequate amount of test material for XRD analysis.

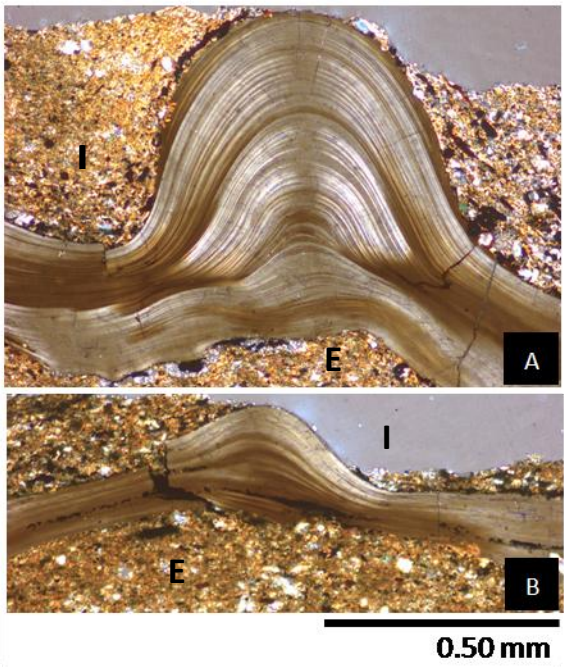

Figure 15- Thin section preparations of transverse sections through parts of the test of specimen RB05 (*Paraconularia* sp.), viewed by transmitted light microscopy in plane polarized light. A) Corner groove internal carina. The earliest lamellar structures to form on the young test (bottom) are rather even. As the conulariid grew the lamellae inflected inward (upward, in this figure) and began to thicken forming the carina. Note that the increased thickness of lamellae in the carina is accompanied by a lighter color, which is again interpreted as an increase in mineralization while organic matrix growth remains constant. B) Midline carinae from the same specimen, showing similar observations. (E = external, I = internal)

Specimens G08, MH02, RB05, and RB08, each representing one of the four species in this study, were analyzed by energy dispersive spectrophometry (EDS) to quantify their elemental compositions. Using the atomic percentages derived from this, stoichiometric procedures were used to determine the possible, and most likely, mineralogical compositions of the conulariid tests.

Two possible mineralogies were considered, one assuming the presesence of two minerals, apatite [$(Ca_5(PO_4)_3)(OH, F)$] and calcite [$Ca(CO_3)$], and the other assuming a single mineral, carbonate-rich apatite [$Ca_5(PO_4,CO_3)_3(OH,F)$]. The absence or abundance of organic material, whether chitin layers or matrix, would be a secondary consideration. Stoichiometric calculations were done for each possibility (Appendix C).

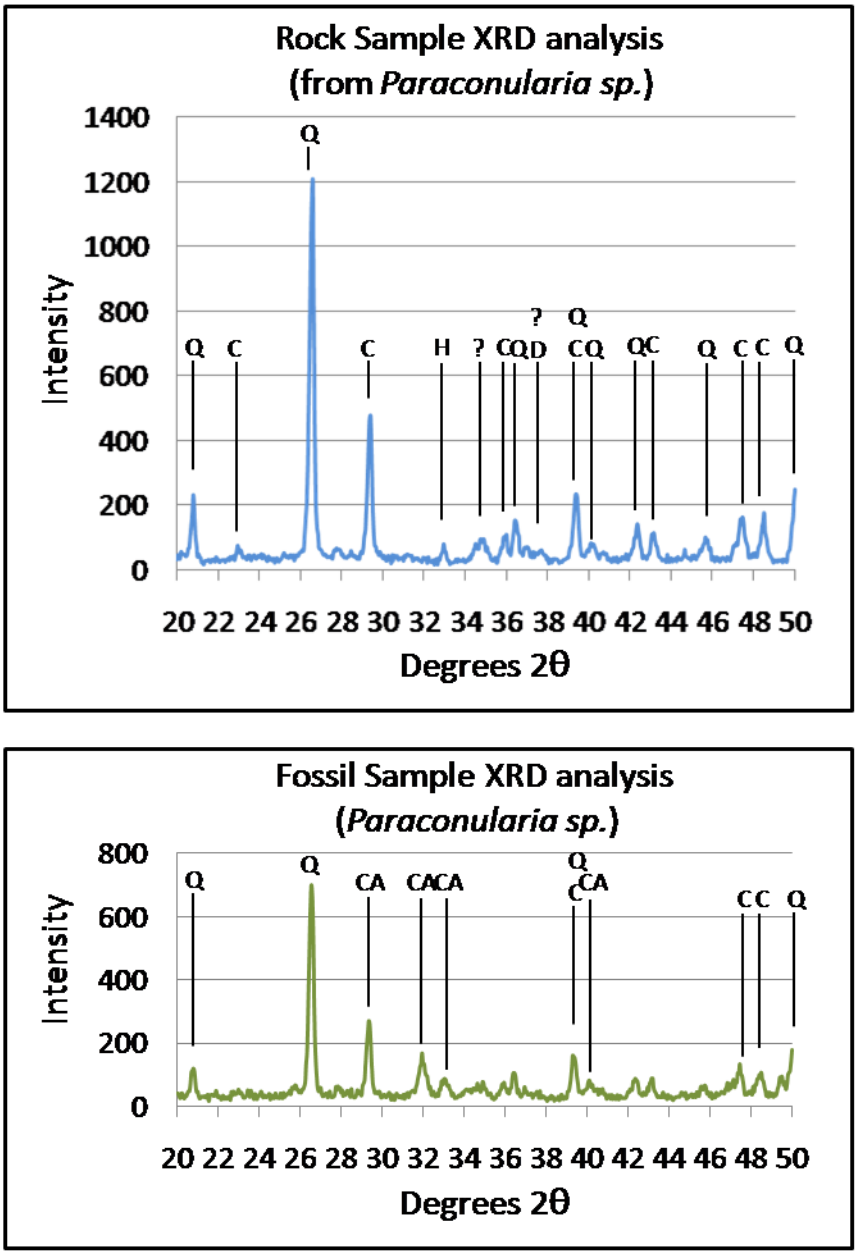

Figure 16- Peak distribution from X-ray Diffraction analysis of (upper chart) rock matrix surrounding a specimen of Paraconularia sp., and (lower chart) fragments of the test and adhered matrix of the same. The matrix sample appears to be composed principally of quartz and calcite, with numerous peaks for each, while the fossil + matrix sample displayed some peaks not found for the matrix, which are in agreement with the peaks expected for carbonate-rich apatite. Unfortunately carbonate-rich apatite shares some peaks with other minerals such as quartz and calcite which can be noted in the graphs above. This leads to a suggestion for carbonate-rich apatite but not a definitive signature. Q= quartz; C= calcite; H= hematite; D= dolomite; CA= carbonate-rich apatite.

These results cannot exclude either possible mineralogy, as all the phosphorous and calcium could be accommodated for either, with the main distinction being in the amount of carbon and oxygen remaining. As there is an abundance of these elements remaining for either set of calculations (presumably present in the organic matter), this is not definitive.

However, the stoichiometric results do indicate a fairly consistent ratio of PO_4 to CO_3 (on the order of 6:1) for the conulariid test. This strongly suggests an orderly arrangement of a single mineral, carbonate-rich apatite, rather than apatite and calcite layering. Alternate layers of two separate minerals would be much more likely to vary in abundance due to environmental constraints.

The stoichiometric results also indicated that specimens MH02, RB05, and RB08 had an average of 37% of the atoms not incorporated into the mineral phase, while, specimen G08 had 62% of its atoms not in the mineral phase. For each specimen, roughly 1/3 of its free atoms are carbon while the remaining 2/3 are oxygen. This is puzzling, as it is closer to the ratios present in carbon dioxide than would be expected in common organic compounds such as the proteins in organic matrix or the sugars present in chitin.

Elemental maps, illustrating the spatial distribution of the elements, were created to determine if there was any observable layering of different mineralogies in the conulariid test. This was done to reaffirm the XRD and stoichiometric results to check if there is any calcitic mineralization layered in the test. The elemental maps displayed a uniform distribution of calcium, phosphorous, and carbon throughout the conulariid test. That supports the result of carbonate-rich apatite mineralogy, and argues against interlayered calcite mineralization in the test.

CHAPTER 4 - Discussion

The primary goal of this study was to determine whether there were significant microstructural and mineralogical variations of the conulariid test associated with different paleoenvironmental settings. The results of the examinations and analyses of the fossil material indicate that there are no obvious paleoenvironmental variations in microstructure and mineralogy among the studied conulariids.

Secondary goals, to determine the conulariid test mineralogy and composition, to determine the presence and distribution of organic matter in the test, and to describe the microstructure of interspaces, transverse ribs, and internal carinae, were also achieved.

Microstructure

During these examinations of the conulariid test an organic matrix was identified for the first time in this group. Although earlier investigators (Moore and Harrington, 1956a; Oliver and Coates, 1987) have speculated on the presence of chitinophosphate, my investigations have shown that the organics are present as a matrix. Another previous study attempted to recover organics by dissolving test fragments in HCl, but failed to identify any (Van Iten, 1992b). The organic matrix is believed to serve as a template for the biomineralization of shells or skeletons. In conulariids the organic matrix seems to distinguish the lamellar structures within the test, by enriching some lamellae with organic matter, and leaving others mostly mineralized. The effect can be seen at the smallest scale in the microlamellae, the most fundamental lamellar structures in the test.

The presence of the organic matrix may also have revealed some phylogenetic details. The fibrous structures that connect the organic-rich microlamellae (Fig. 8) may be additional

evidence to further support a coronatid scyphozoan affinity. These structures appear to be analogous to the structures described in the *Stephanoscyphus* (Scyphozoa, Coronatae) periderm by Chapman and Werner (1972). Chapman and Werner (1972) described the coronate lamellae as being separated by gaps bridged by minute processes. That description is very similar to my observations of conulariid organic matrix and microstructure.

It has been accepted by most workers that the conulariid test is constructed by the addition of lamellae to the interior test wall. The only problem is that the term lamella has been used to describe lamellar structures of all different sizes in the conulariid test. It became evident in my observations that there was a need to distinguish between, and to understand the types of, lamellae. I do not wish to needlessly add new anatomical terminology to an already extensive paleontological lexicon, but I have found the terms microlamellae, mesolamellae, and macrolamellae useful in this study to distinguish between the different (but related) lamellar features seen within conulariid test.

Large discrepancies between lamellae size have been noted before, and explained as being variation between species (Brood, 1995). That may be the case, but based upon the results gathered in this study it is very possible that the discrepancies may be because previous reports were inconsistent in their designations of lamellar structures. The earlier research (Barrande, 1867; Bouček and Ulrich, 1929; Moore and Harrington, 1956a) and some later work (Kozlowski, 1968; Bischoff, 1978; Brood, 1995) on conulariid test microstructure were undertaken using transmitted light microscopy. Based on my results these works were describing macrolamellae characteristics. Mesolamellae may have been described as well, but as these are only visible using crossed polarized transmitted light, and as this is only common in petrographic microscopes, it seems unlikely.

Later workers (Chapman, 1966; Werner, 1966a, 1967; Van Iten, 1991a, b, 1992a, b) examined the conulariid microstructure almost exclusively with scanning electron and transmitted electron microscopy, and these reports may have been interpreting a combination of macrolamellae and microlamellae characteristics. Most of the previous research done with the SEM was done on polished sections. Without etching the conulariid test it is extremely difficult to make out the smallest microlamellae (unless natural dissolution between microlamellae in the test has occurred). Macrolamellar characteristics can still be seen even on polished sections (Fig. 19). Some 'dense' and 'vacuity-bearing' lamellae observed in polished sections described by Kozlowski (1968), Bischoff (1978), and Van Iten (1992b) may be caused by the organic-rich lamellar structures being preferentially removed by the polishing agent due to its softer nature than the organic-poor (more mineralized) microlamellae dominated lamellar structures. Therefore the 'dense' lamellae may represent more mineralized portions of the test, and the 'vacuity-bearing' lamellae are more organic-rich. The consequence of this possibility is that the previous works done with polished sections may

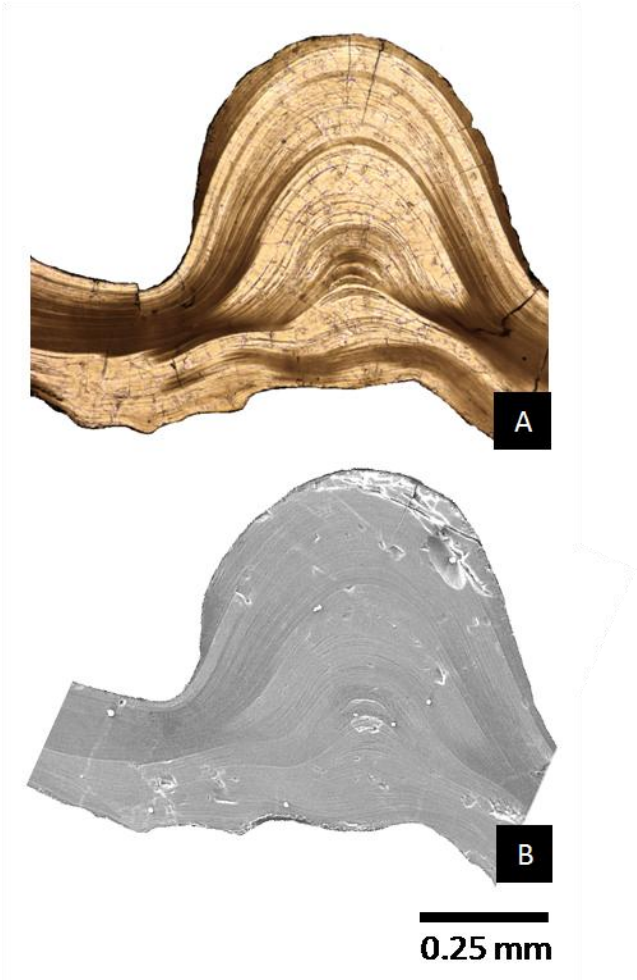

Figure 17- Transverse sections through the corner groove carinae of specimen RB05 (*Paraconularia* sp.) A) Thin section preparation viewed by transmitted light microscopy, using plane polarized light. B) Etched and critical-point dried preparation imaged by scanning electron microscopy. The dark-colored macrolamellae of (A) match up perfectly with the dark colored macrolamellae in (B), as do the light-colored macrolamellae.

be opposite to the results of etched sections. In the etched section of the conulariid test the 'dense' lamellar structures were organic-rich and the 'vacuity-bearing' lamellar structures were more mineralized.

Van Iten (1992b) described the growth of the transverse ribs, and internal carinae (test thickenings) as "gradual, symmetrical thickening of individual lamellae". Based upon the results acquired for this report, that conclusion is generally true, but there is some expansion that needs to be done to better understand the test building process. In Figure 14 two zones of microlamellar growth are shown in outline. In Zone I it appeared that mineralization was the main contributor to test thickening in that rib. In Zone II the mineralization appeared to be reduced and organic matrix growth was the main contributor. According to Clark (1999) that pattern may have been caused by a more continuous organic growth, even when mineral growth is slowed or stopped. This may be reflected in the mesolamellae and macrolamellae with the thickening and thinning of certain features. Such differences in organic content and overall thickness may have been caused by environmental stresses (Clark 1974, 1999). For example when the dark colored macrolamellae are traced into a test thickening they often fan out and appear to dilute their organic content due to an increase in mineralization rate. On the other hand the light colored lamellae may thicken, and the opposite can be observed when the lamellae are traced back into an interspace.

The macrolamellae present in *Paraconularia sp.* specimens RB01 and RB05 may represent environmentally induced stresses. Even though the organic matrix construction mechanisms do not appear to be affected by the environment, the amount of biomineralization appears to be. The environment did not change the mineralogy, but may have altered the growth rate (this will be further explained in the following section). Clark (1974) describes two types of

events that influence shell growth, periodic and random. Periodic events can be daily, lunar, tidal, or seasonal cycles. Random events can be caused by storm events, turbidity, temperature, predatory attacks, etc. Specimen RB01, which has a rather uniform distribution of light and dark colored macrolamellae, may display periodic growth lines with little random environmentally induced stresses (Fig. 12). Specimen RB05, however, has a clustered, uneven distribution of light and dark colored macrolamellae, suggesting a more random event influence on its growth history. The thick clustering of dark colored macrolamellae may represent a period of environmentally induced stress that reduced the biomineralization process allowing for the growth of more organic-rich lamellar structures.

Mineralogy

Biomineralization requires a space or compartment to provide a local environment that can become supersaturated with one or more mineral phases (Clark, 1976; Dove, 2010). These compartments control ion flow and composition to create the necessary environment to produce mineralization. It is this isolation from the seawater and ionic control that makes determining the paleoenvironment difficult based upon test mineralization alone. One main environmental factor that can affect the biomineralization process is a limited abundance of the required ions that would be used in biomineralization. According to Dove (2010) there are two ways organisms can deal with this issue: first, they can use fewer of the required ions (for conulariids it would be PO_4) in their skeletons, and secondly, they can migrate (if mobile) or colonize new environments abundant with their required ions. Isotope and trace element studies may be a better indicator of environmental influences upon the test composition, and that would be a great follow-through for future research.

There is no distinguishable mineralogical variation present in the conulariid tests to determine paleoenvironmentally influenced differences. The mineralogical results derived from the XRD and EDS analyses suggest carbonate-rich apatite, or less probably a physical mixture or alternating layers of apatite and calcium carbonate, as the mineral constituent in the conulariid test. This supports Van Iten's (1992b) report. The other published mineralogical possibilities, such as apatite (Moore and Harrington, 1956a; Babcock and Feldmann, 1986b), and chitinophosphate (Moore and Harrington, 1956a; Oliver and Coates, 1987) do not appear as likely, based upon the results. According to Carter (1990) pure apatite does not commonly occur in nature, and has not been observed to form biogenically. Based on Carter's (1990) research pure apatite is a very unlikely option. Starynkevitch and Belov (1940, 1953), Bacquet et al. (1980), and Nathan (1984) have determined that natural apatites usually contain some percentage of carbonate anions in the apatite crystal lattice substituting for phosphate anions. If this is true this would also support this project's findings and Van Itens's (1992b) of a carbonate-rich apatite test mineralogy.

Chitinophosphate is an organic substance comprised of chitin that is either alternating with or impregnated with phosphatic mineralization (Allaby, 1999). True chitin is a major component of insect exoskeletons and has a composition unlike the organic matrix found in most other invertebrates. Chitin cannot be rejected based on the analyses conducted here, but seems unlikely given the obvious presence of an organic matrix, which in itself can account for the high levels of carbon observed.

CHAPTER 5 - Conclusion

There was no significant microstructural variability observed in the conulariid tests of different species or from varying paleoenvironmental settings. All the examined specimens demonstrated great similarity in several types of test features.

Distinction between three types of lamellae (microlamellae, mesolamellae, and macrolamellae) can be important in the clarification of potential discrepancies among older, newer, and sometimes contemporary literature. The different types of lamellae can be seen by different methods. The microlamellae are best observed in etched specimens prepared for the SEM. Mesolamellae are only seen when test sections are viewed with transmitted cross polarized light, and the macrolamellae are best observed in transmitted plane polarized or unpolarized light microscopy. The microlamellae are the smallest lamellar structures that group together to form the larger lamellar structures. The mesolamellae and macrolamellae can be further distinguished into the organic-rich lamellae (darker color) and organic-poor lamellae (lighter color).

The lamellar thickening in the formation of test thickenings generally supports Van Iten's (1992b) previous interpretations. The added information gave more detail into how this occurred with either more mineralogical influenced thickening or organic influenced thickening possibly depending upon environmental stresses.

Etched specimens that are processed by critical point drying can reveal and preserve the organic matrix. Observations of the organic matrix revealed that fibrous structures bridge the gaps left by the dissolution of the organic-poor microlamellae, connecting the organic-rich microlamellae. That description is analogous to Chapman and Werner's (1972) description of a

coronate scyphozoan periderm microstructure. This observation is another line of evidence strengthening the case for a conulariid and coronate scyphozoan relationship.

There is no mineralogical variation in the conulariid tests to support paleoenvironmental differences. The XRD and EDS analyses done on the conulariid test suggested a carbonate-rich apatite composition supporting Van Iten's (1992b) findings.

References

Allaby, M., 1999, "Chitinophosphatic." A Dictionary of Zoology. Oxford University Press.

Ausich, W.I., and Meyer, D.L., 1990, Origin and composition of carbonate buildups and associated facies in the Fort Payne Formation (Lower Mississippian, South-Central Kentucky): an integrated sedimentologic and paleoecologic analysis. Geologic Society of America Bulletin, v. 102, p.129-146.

Babcock, L.E., and Feldmann, R.M., 1986a, The phylum Conulariida. In: A. Hoffmann and M.H. Nitecki (eds.). Problematic fossil taxa, Oxford University Press, Oxford, pp. 135-147.

Babcock, L.E., and Feldmann, R.M., 1986b, Devonian and Mississippian Conulariids of North America. Annal of Carnegie Museum, v. 55, p. 349-479.

Barrande, J., 1867, Systéme silurien du centre de la Bohême. Ière Paratie. Tome 3. Classe des Mollusques, Ordre des Ptéropods. Prague and Paris, p. 179.

Bischoff, G.C.O., 1978, Internal structures of conulariid tests and their functional significance, with special reference to the Circoconulariina n. suborder (Cnidaria, Scyphozoz): Senckenbergiana Lethaia, v. 59, p. 275-327.

Bouček, B., 1939, Conulariida. In: O. H. Schindewolf (ed.). Handbuch der Palaezoologie, Germany, p. 111-131.

Bouček, B., and Ulrich, F., 1929, Étude sur la coquille du genre *Conularia* Miller. Statniho geologickehou ustavu Ceskoslovenske Respublicky, Vestnik, v. 5, p. 1-25.

Brood, K., 1995, Morphology, structure, and systematic of the conulariids: GFF, v. 117, p. 121-137.

Carter, J.G., 1990, Skeletal Biomineralization: Patterns, Processes and Evolutionary Trends (eds.), New York.

Chapman, D.M., 1966, Evolution of the scyphistoma. In the Cnidaria and Their Evolution (ed. W.J. Rees), p. 51-75. London: Academic Press.

Chapman, D.M., and Werner, B., 1972, Structure of a solitary and colonial species of *Stephanoscyphus* (Scyphozoa, Coronata) with observations on periderm repair. Helgoländer Wissenschaftliche Meeresuntersuchungen, v. 23, p. 393-421.

Clark, G.R., 1974, Growth lines in invertebrate skeletons: Annual Review of Earth and Planetary Sciences, v. 2, p. 77-99.

Clark, G.R., 1976, Shell growth in the marine environment: Approaches to the problem of marginal calcifications: Journal of American Zoology, v. 16, p. 617-626.

Clark, G.R., 1999, Microstructural transitions in the shells of *Mercenaria mercenaria* as functions of age and stress. Geological Society of America Abstracts and Programs, v. – p. A471.

Clark, G.R., Rhoads, D.C., and Lutz, R.A., 1980, Techniques for observing the organic matrix of molluscan shells: Skeletal Growth of Aquatic Organisms. Plenum Publishing Corporation.

Dosen, A., 2009, Mineralogical studies of phase transitions and disorder in Ca-phosphates: brushite and biologic apatite: Ph. D. dissertation, Graduate School of University at Buffalo, State University of New York. UMI dissertation publishing, Ann Arbor, MI.

Dove, P.M., 2010, The rise of skeletal biominerals: Elements, v. 6, p. 37-42.

Feldmann, R.M., and Babcock, L.E., 1986, Exceptionally preserved conulariids from Ohio-reinterpretation of their anatomy. National Geographic Research, v. 2, p. 464-472

Kinderlen, H., 1937, Die Conularien. Über Bau and Leben der ersten Scyphozoa. Neus Jahrbuch für Mineralogie, Beilage- Band, v. 77, p. 113-169.

Kozlowlski, R., 1968, Nouvelles observations sur les conulaires. Acta Palaeontologica Polonica, v. 13, p. 497-535.

Krause, R.A., Jr., and Meyer, D.L., 2004, Sequence stratigraphy and depositional dynamics of carbonate buildups and associated facies from the Lower Mississippian Fort Payne Formation of Southern Kentucky, U.S.A.. Journal of Sedimentary Research, v. 74, p. 831-844.

Leme, J.M., Rodrigues, S.C., Simões, M.G., and Van Iten, H., 2004, Sistemática dos conurlários (Cnidaria) da Formação Ponta Grossa (Devoniano), do Estado do Paraná, Brasil. Revista Grasileira de Paleontologia, v. 7, p. 213-222.

Leme, J.M., Simões, M.G., Rodrigues, S.C., Van Iten, H., and Marques, A.C., 2008, Major developments in conulariid research: problems of interpretation and future prospective. Ameghiniana, v.45, p. 407-420.

Meyer, D.L., Ausich, W.I., and Richard, T.E., 1989, Comparative taphonomy of echinoderms in carbonate facies: Fort Payne Formation (Lower Mississippian) of Kentucky and Tennessee: Palaios, v. 4, p. 533-552.

Moore, R.C., Harrington, H.J., 1956a, Conulata. *In*: R.C. Moore (ed), Treatise on Invertebrate Paleontology: Part F: Coelenterata, Geological Society of America and University of Kansas, New York and Lawrence, p. F27-F38.

Moore, R.C., Harrington, H.J., 1956b, Conulata. *In*: R.C. Moore (ed), Treatise on Invertebrate Paleontology: Part F: Coelenterata, Geological Society of America and University of Kansas, New York and Lawrence, p. F54-F66.

Oliver Jr., W.A., and Coates, A.G., 1987, Phylum Cnidaria. *In*: Boardman, R.S., Cheetham, A.H., and Rowell, A.J., (ed.) Fossil Invertebrates. Blackwell Scientific Publications, Palo Alto, Oxford, p. 192.

Pryor, W.A., Sable, E.G., 1974, Carboniferous of the Eastern Interior Basin, *in* Briggs, G., Carboniferous of the southeastern United States: Geological Society of America Special Paper 148, p. 281-313.

Raatz, W.D., and Ludvigson, G.A., 1996, Depositional environments and sequence stratigraphy of Upper Ordovician epicontinental deep water deposits, eastern Iowa and southern Minnesota. Geological Society of America, Special Publication 306, p. 143-159.

Reed, F.R.C., 1933, Some new species of *Conularia* from Girvan. Geological Magazine, v. 70, p. 354-358.

Simões, M.G., Mello, L.H.C., Leme, J.M., Rodrigues, S.C., and Marques, A.C., 1999, Devonian conulariid taphonomy and their paleoecological implications. Geological Society of America, Abstracts A-468.

Steul, H., 1984, Die systematishce Stellung der Conularien. Giessener Geologische Schriften, v. 37, p. 117.

Van Iten, H., 1991a, Evolutionary affinities of conulariids. In: A.M. Simonetta and S.C. Morris (Eds.): The early evolution of Metazoa and the significance of problematic fossil taxa. Cambridge University Press, Cambridge, p. 145-154.

Van Iten, H., 1991b, Anatomy, pattern of occurrence, and nature of the conulariid schott: Paleontology, v. 34, p. 939-954.

Van Iten, H., 1992a, Anatomy and phylogentic significance of the corners and midlines of the conulariid test: Palaeontology, v. 35, p. 335-358.

Van Iten, H., 1992b, Microstructure and growth of the conulariid test: implications for conulariid affinities: Palaeontology, v. 35, p. 359-372.

Van Iten, H., 1994, Redescription of *Glyptoconularia* Sinclair, an Ordovician conulariid from North America. In: E. Landing (de.), Studies in Honor of Donald W. Fisher, New York State Museum and Geological Survey, Bulletin 481, p. 363-366.

Van Iten, H., Fitzke J.A., and Cox, R.S., 1996, Problematical fossil Cnidarians from the upper Ordovician of the North-Central USA: Palaeontology, v. 39, p. 1037-1064.

Van Iten, H., Zhu, Z.K., Zhu, M.Y., 2000, Anatomy and systematic of the Devonian conulariids *Changshaconus* Zhu, 1985 and *Reticulaconularia* Babcock and Feldmann, 1986. Acta Palaeontologica Sinica, v. 39, p. 466-475.

Van Iten, H., Vhylazova, Z., Mao-yan, Z., and Qian, Y., 2005a, Widespread occurrence of microscopic pores in conulariids. Journal of Paleontology, v. 79, p. 400-407.

Van Iten, H., Leme, J.M., Rodrigues, S.C., and Simões, M.G., 2005b, Reinterpretation of a conulariid-like fossil from the Vendian of Russia. Palaeontology, v. 48, p. 619-622.

Van Iten, H., Leme, J.M., and Simões, M.G., 2006a, Additional observations on the gross morphology and microstructure of *Baccaconularia* Hughes, Gunderson et Weedon, 2000, a Cambrian (Ferongian) conulariid from the north-central USA. Palaeoworld, v. 15, p. 294-306.

Van Iten, H., Leme, J.M., Rodrigues, S.C., and Simões, M.G., 2006b, New data on the anatomy of *Conularia Milwaukeensis* Cleland, 1911 (Middle Devonian, Iowa and Wisconsin). Journal of Paleontology, v. 80, p. 393-395.

Werner, B., 1966a, *Stephanoscyphus* (Scyphozoa, Coronata) und seine direkte Abstammung von den fossilien Conulata. Helgoländer Wissenschaftliche Meeresuntersuchungen, v. 13, p. 317-347.

Werner, B., 1966b, Morphologie, Systematik und Lebensgeschichte von *Stephanoscyphus* (Scyphozoa, Coronatae) sowie seine Bedeutung für die Evolution der Scyphozoa. Verhandlungen der Deutschen Zoologischen Gesellschaft in Göttingen, Zoologischer Anzeiger Supplement, v. 30, p. 397-319.

Werner, B., 1967, *Stephanoscyphus* Allman (Scyphozoa, Coronatae), ein rezenter Vertreter der Conulata? Paläontologische Zeitschrift, v. 41, p. 137-153.

Witzke, B.J., 1980, Middle and Upper Ordovician paleogeography of the region bordering the Transcontinental Arch. 1-18. *In* Fouche, T.D., and Magathan, E.R., (eds.), Paleozoic paleogeography of the west-central United States. Society of Economic Paleontologists and Mineralogists, Rocky Mountain Section, Denver, Colorado, p. 431.

Witzke, B.J., 1987, Models for circulation patterns in epicontinental seas applied to Paleozoic facies of North American Craton. Paleoceanography, v. 2, p. 229-248.

Witzke, B.J., and Glenister, B.F., 1987, Upper Ordovician Maquoketa Formation in the Graf area, eastern Iowa. 103-108. *In* Biggs, D.C., (ed.). Geological Society of America Centennial Field Guide, North-Central Section, p. 448.

Appendix A - Collection Localities

The Maquoketa Formation, Elgin Member sites were selected from Van Iten et al. (1996) with the exceptions of the Decorah and Cow Creek sites. The Fort Payne Formation sites are from unpublished locations, and they were not previously known to produce conulariids.

Maquoketa Formation, Elgin Member

1) Graf, Dubuque County, Iowa (42° 29’ 20.15” N, 090° 52’ 33.08”W): graptolite shales and mixed faunas biofacies; road-cut on northwest side of gravel road 0.4 km southwest of Graf.
2) Montauk Hill, Clermont, Fayette County, Iowa (43° 00 ’23.83” N, 091° 38’ 55.80” W): trilobite dominated biofacies; road-cut on southeast side of Highway 18 near base of Montauk Hill.
3) Elgin, Fayette County, Iowa (42° 57’ 09.63” N, 091° 36’ 25.02” W): trilobite dominated biofacies; road-cut on northeast side of County Road B64, about 1.6 km east-southeast of Elgin along the Fayette / Clayton County line.
4) Elgin, Clayton County, Iowa (42° 56’ 20.79” N, 091° 35’ 33.28” W): trilobite dominated biofacies; cow creek bank and creek bottom on south side of Abbey Road approximately 4 km southeast of Elgin.
5) Decorah, Winneshiek County, Iowa (43° 18’ 03.70” N, 091° 48’ 49.62” W): Galena Group, road-cut on northwest side of junction of Highway 52 / State Highway 9
6) Granger, Fillmore County, Minnesota (43° 30’ 37.67” N, 092° 08’ 55.11” W): brachiopod - echinoderm dominated biofacies; road-cut approximately 0.5 km west-northwest of Granger.
7) Rifle Hill, Fillmore County, Minnesota (43° 36’ 04.69” N, 092° 14’ 31.49” W): brachiopod - echinoderm dominated biofacies; road-cuts approximately 11 km east of junction of Highway 63 / Fillmore County Road 14.

Fort Payne Formation

1) Cheatham Dam, Cheatham County, Tennessee (36° 19’ 06.12” N, 087° 11’ 50.60” W): siltstone and sheet-like packstone facies; railroad track approximately 0.2 km west of Cheatham Dam Road before it splits.
2) Fox Bluff, Cheatham County, Tennessee (36° 18’ 56.17” N, 087° 11’ 09.50 W): siltstone facies; railroad track approximately 0.1 km east-northeast Cheatham Dam campground.
3) Ashland City, Cheatham County, Tennessee (36° 14’ 40.92” N, 087° 02’ 01.03” W): siltstone and fossiliferous green shale facies; abandoned quarry 0.5 km southwest of Highway 12.
4) Ashland City, Cheatham County, Tennessee (36° 13’ 49.18” N, 087° 00’ 08.96” W): fossiliferous green shale facies; found in float in what was a construction site that is located around Eisenhower Drive in the Caldwell Subdivision.
5) Scottsboro, Davidson County, Tennessee (36° 12’ 29.05” N, 088° 57’ 29.85” W): fossiliferous green shale facies; road cuts on River Trace 3.3 km west of Scottsboro.

Appendix B - Prepared Specimens

Specimen No.	*Genus / Species*	Site No.	Thin Section (Trans.)	Thin Section (Long.)	SEM (Trans.)	SEM (Long.)
Maquoketa Formation, Elgin Member (Richmondian, Ordovician)						
G08	*Conularia trentonensis*	1	X	X	X	X
G11	*C. trentonensis*	1	X		X	
CC01	*C. splendida*	4	X	X	X	X
MH02	*C. splendida*	2	X	X	X	X
Fort Payne Formation (Osagean, Mississippian)						
RB01	*Paraconularia sp.*	4	X	X	X	X
RB05	*P. species*	4	X	X	X	X
RB06	*P. missouriensis*	1				X
RB07	*P. missouriensis*	1		X		X
RB08	*P. missouriensis*	1		X		X
RB09	*Paraconularia sp.*	5	XRD Analysis			

Table 1- Prepared specimens for use in variaous examinations and analysis.

Appendix C - Stoichiometry

		Measured	Assigned P	Left	Assigned C	Left	Assigned F	Left
RB05	P	7.57	7.57	0.00	-	0.00	-	0.00
	Ca	14.6	12.6	2.00	2.00	0.00	[14.6]	0.00
	C	12.9	-	12.9	1.20	11.7	-	11.7
	O	61.2	30.3	30.9	3.6	27.3	-	27.3
	F	3.86	-	3.86	-	3.86	2.92	0.94
RB08	P	7.93	7.93	0.00	-	0.00	-	0.00
	Ca	15.3	13.2	2.1	2.10	0.00	[15.3]	0.00
	C	12.4	-	12.4	1.24	11.2	-	11.2
	O	61.2	31.7	29.5	3.71	25.8	-	25.8
	F	3.26	-	3.26	-	3.26	3.06	0.20
G08	P	4.78	4.78	0.00	-	0.00	-	0.00
	Ca	9.20	7.98	1.22	1.22	0.00	[9.20]	0.00
	C	21.3	-	21.3	0.73	20.6	-	20.6
	O	64.2	19.1	45.1	3.66	41.4	-	41.4
	F	0.54	-	0.54	-	0.54	(1.84)	0.00
MH02	P	8.05	8.05	0.00	-	0.00	-	0.00
	Ca	15.7	13.4	2.3	2.3	0.00	[15.7]	0.00
	C	11.7	-	11.7	1.38	11.3	-	11.3
	O	60.8	32.2	28.6	6.9	21.7	-	21.7
	F	3.75	-	3.75	-	3.75	3.14	0.61

Table 2- The stoichiometric procedures for carbonate-rich apatite.